Hindawi Publishing Corporation
Journal of Nanomaterials
Volume 2015, Article ID 979561, 10 pages
http://dx.doi.org/10.1155/2015/979561

Research Article

Effect of Graphene and Fullerene Nanofillers on Controlling the Pore Size and Physicochemical Properties of Chitosan Nanocomposite Mesoporous Membranes

Irene S. Fahim,[1,2] Narguess Marei,[1] Hanadi G. Salem,[1,2] and Wael Mamdouh[1,3]

[1] *Yousef Jameel Science and Technology Research Center (YJSTRC), School of Sciences and Engineering (SSE), The American University in Cairo (AUC), AUC Avenue, P.O. Box 74, New Cairo, Cairo 11835, Egypt*
[2] *Department of Mechanical Engineering, School of Sciences and Engineering (SSE), The American University in Cairo (AUC), AUC Avenue, P.O. Box 74, New Cairo, Cairo 11835, Egypt*
[3] *Department of Chemistry, School of Sciences and Engineering (SSE), The American University in Cairo (AUC), AUC Avenue, P.O. Box 74, New Cairo, Cairo 11835, Egypt*

Correspondence should be addressed to Wael Mamdouh; wael_mamdouh@aucegypt.edu

Received 27 November 2014; Accepted 28 January 2015

Academic Editor: Stefan I. Voicu

Chitosan (CS) nanocomposite mesoporous membranes were fabricated by mixing CS with graphene (G) and fullerene (F) nanofillers, and the diffusion properties through CS membranes were studied. In addition, in order to enhance the binding between the internal CS chains, physical cross-linking of CS by sodium tripolyphosphate (TPP) was carried out. F and G with different weight percentages (0.1, 0.5, and 1 wt.%) were added on physically cross-linked chitosan (CLCS) and non-cross-linked chitosan (NCLCS) membranes by wet mixing. Permeability and diffusion time of CLCS and NCLCS membranes at different temperatures were investigated. The results revealed that the pore size of all fabricated CS membranes is in the mesoporous range (i.e., 2–50 nm). Moreover, the addition of G and F nanofillers to CLCS and NCLCS solutions aided in controlling the CS membranes' pore size and was found to enhance the barrier effect of the CS membranes either by blocking the internal pores or decreasing the pore size. These results illustrate the significant possibility of controlling the pore size of CS membranes by cross-linking and more importantly the careful selection of nanofillers and their percentage within the CS membranes. Controlling the pore size of CS membranes is a fundamental factor in packaging applications and membrane technology.

1. Introduction

Particle pollution, also known as particulate matter (PM), includes the very fine dust, soot, smoke, and droplets that are formed from chemical reactions and produced when fuels such as coal, wood, or oil are burned. Particles may also come from fireplaces, wood stoves, unpaved roads, and crushing and grinding operations and may be blown into the air by the wind. US Environmental Protection Agency (EPA) scientists and other health experts are concerned about particle pollution because very small or "fine" particles can get deep into the lungs. These fine particles, by themselves, or in combination with other air pollutants, can cause increased emergency room visits and hospital admissions for respiratory illnesses and tens of thousands of deaths each year. They can aggravate asthma, cause acute respiratory symptoms such as coughing, reduce lung function resulting in shortness of breath, and cause chronic bronchitis. The particle size of these pollutants ranged from 2 to 50 nm. So the need for separation membranes is crucial nowadays to meet this unforeseen danger [1, 2].

Membrane technology attracted increasing attention in the past few years mainly due to the unique ability to control the membrane's pore size and its barrier properties. Current research on membranes focuses on polymeric membranes due to the optimum control of the pore forming mechanism, higher flexibility, and mechanical strength. Polymers also exhibit a huge range of mass transport properties depending

on the type of polymer, additives, and fillers, production process used, and the end purpose [3]. In addition, the incorporation of nanofillers into polymeric membranes has been a trend to overcome some of the existing disadvantages such as chemical incompatibilities with process solutions and temperature limitations. Careful experimental studies in order to select the most appropriate type and composition of nanofillers polymeric membranes were reported [4].

There are several types of separation membranes that can be utilized to filter these industrial pollutants. Porous membranes are classified into several kinds by their size. According to International Union of Pure and Applied Chemistry (IUPAC) notation, microporous membranes have pore diameters of less than 2 nm and macroporous materials have pore diameters of greater than 50 nm; the mesoporous category lies between 2 and 50 nm [2].

Several polymers that are commonly used as separation membranes and packaging such as nylon, low-density polyethylene (LDPE), polytetrafluoroethylene (PTFE), and chitosan have been reported. Nylon membranes were fabricated with pore sizes ranging from 200 to 450 nm at a yield tensile strength of 70 MPa [5]. LDPE membranes on the other hand, were reported to have pore sizes in the range of 40–70 nm with a yield tensile strength of 65 MPa [6]. In addition, PTFE membranes were fabricated with pore sizes ranging from 10 to 30 nm at a yield strength of 57 MPa [7].

Previous studies on the formulation of selective natural or synthetic permeable membranes with pore size between 0.2 μm and 1.2 μm were reported [8]. Plackett et al. used cellulose as a natural material for membranes industry. The nanostructure of cellulose played a significant part in improving the membrane mechanical and barrier properties [9, 10]. Chitosan was used to fabricate CS membranes with high porosity and good mechanical properties using silica particles as porogen. By controlling the size of the silica particles (5, 10, and 15–40 μm), the desired pore size was produced [11].

Chitosan is a natural polymer and it is the deacetylated form of chitin that showed a great potential as a natural material compared to cellulose in preparing polymeric membranes, due to its biocompatibility and relatively low toxicity [12, 13]. One of chitosan's most important features is the ability to be shaped into different forms such as fibers, hydrogels, beads, sponges, and membranes [13]. Chitosan was used in several agricultural, food preservation, biomedical, and biotechnological applications. The most vital importance is the film-forming property of chitosan which made it a potential industrial source as food preservative or coating material in drug manufacturing [14]. Chitosan has been used in the preparation of membranes and has also been incorporated into other packaging materials. On the other hand, chitosan was incorporated as an antimicrobial additive into low density polyethylene (LDPE) with different concentrations. These chitosan incorporated films were applied on red meat surfaces which enhanced the microbial growth inhibition [15].

Cross-linking of chitosan has been reported to result in the formation of chitosan nanofillers which exhibit unique properties at the nanoscale regime compared to the non-cross-linked chitosan [3]. Factors affecting physical cross-linking of polymers vary from the type, concentration of the cross-linking agent, and the cross-linking time. Higher concentrations of cross-linking agent were reported to induce rapid physical cross-linking process [16].

Nanofillers have been widely used as reinforcements to enhance the physical and morphological properties of polymers. One of the most interesting reinforcement materials is graphene which is considered as a promising nanofiller due to its excellent mechanical, thermal, and electrical property, combining with its ultrahigh surface area and economical sources. Therefore, G has been widely used in improving the barrier effect of polymeric membranes by blocking the pores and enhancing tensile strength of membranes. There are several structures of graphene including, 0-D fullerenes made by wrapping a section of graphene sheet [17]. Graphene has an affinity to organic compounds and polymers due to the presence of multipores, functional acids, and OH groups on its surface [18]. Fullerene on the other hand is another carbon allotrope. They are closed hollow cages consisting of carbon atoms interconnected in pentagonal and hexagonal rings. Their unique properties are a result of the high symmetry of the nanoarchitectures and the presence of novel π-conjugated systems in them. Fullerenes form a wide variety of donor-acceptor complexes with different classes of organic donors. These complexes show a wide range of mechanical and physical properties that have tremendous potential as building blocks for new nanocomposite materials [19].

Polymer nanocomposites (PNC) membranes are the future for the global packaging industry. This is due to the presence of nanofillers in the polymer matrix materials which improve the packaging properties of the polymer nanocomposite membranes such as flexibility, gas barrier, temperature/moisture stability, thermal stability, recyclability, dimensional stability, heat resistance, and optical clarity. Filler particles can influence the molecular absorption behaviour in two principal ways, where the solubility of the filler differs from the polymer matrix; then the absorption can be either increased or decreased depending on the relative solubility of the molecule in the matrix and filler. Most common inorganic filler particles (e.g., glass or carbon fibres, talc, clays, and silica) can usually be considered as impermeable in comparison to polymer matrix. The presence of nanofillers can also affect the diffusion behaviour. Diffusing molecules would need to work their way around impermeable particles, increasing path lengths and reducing mass transport rates. Improved barrier properties from nanofillers would be expected from the increased lengths of diffusion paths [20].

2. Materials and Experimental Procedure

2.1. Materials and Preparation. Shrimps' shells were purchased from the Egyptian local market. Chitin was extracted from shrimp shells [21]. Shrimps' shells were deproteinized by boiling repetitively in a solution of 1N NaOH in multisequential steps and demineralised using 1N HCl. Chitin was deacetylated using 20% NaOH to obtain chitosan. This % of acetylation was chosen as chitosan exhibits the highest structural charge density at this acetylation %. Chitosan displays polyelectrolyte behaviour related to long-distance

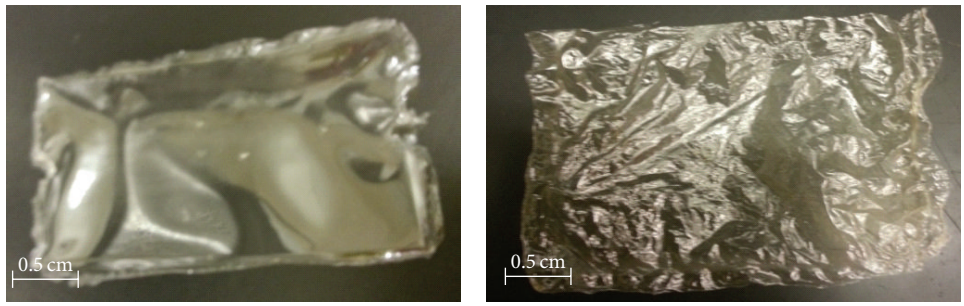

(a) (b)

Figure 1: Pictures of fabricated (a) NCLCS and (b) CLCS membranes, respectively.

intra- and intermolecular electrostatic interactions, which are responsible for chain expansion, high solubility and ionic condensation [22]. All chemicals were purchased from Sigma Aldrich. Sodium hydroxide (NaOH) and hydrochloric acid (HCl) were used in the extraction process of chitosan from shrimp shells acetic acid (Ac-OH, 99% purity) used for dissolving chitosan. Ethanol (99.5% purity) was used for chitosan film fixation. Methanol (99.9% purity) was used for cleaning glassware. Sodium tripolyphosphate (TPP) was used to synthesize chitosan nanoparticles. Phenolphthalein (phph, 99% purity) was used as an indicator for NaOH for testing permeability of membranes.

To prepare the CLCS membranes, 0.2 gm of chitosan (CS) was dissolved in 2% acetic acid at room temperature with continuous stirring. One type of physical cross-linking agent (TPP) was used in this study. 0.033 gm TPP was dissolved in 11 mL distilled H_2O and was added drop-wise onto the CS solution during the homogenization at 10,000 rpm for 30 min using a Polytron homogenizer PT 10-35 GT.

Graphene (Sky spring Nanomaterials, Inc., USA) was used to produce the NCLCS/G and CLCS/G membranes with different G wt.%. The G particle size is 6–8 nm. Fullerene (carbon 60, 99.5+%, 25 gm SES Research, USA) was used to produce the CLCS/F and NCLCS/F membranes with different F wt.%. The F particle size is (0.7–1 nm). Methanol (Sigma Aldrich, 99.9% purity) was used for cleaning the glassware.

2.2. Film Processing. CLCS and NCLCS solutions were mixed with two nanofiller (G and F) with 0.1, 0.5, and 1 wt.% by solvent mixing. Mixing occurs with constant stirring for 60 min with VWR Standard analogue Shaker, to form a clear homogeneous solution. The solutions were used to produce NCLCS/G, NCLCS/F, CLCS/G, and CLCS/F nanocomposite membranes. The NCLCS and CLCS filtrate were poured into two separate flattened containers and left to dry at room temperature to form CS membranes with 0.5 mm thickness. The dry membranes obtained from NCLCS and CLCS solutions are shown in Figure 1. The same procedure was used for the CLCS/G, CLCS/F, NCLCS/G, and NCLCS/F. The process of membrane casting is reproducible.

2.3. Morphological Characterization. The microstructure of the NCLCS and CLCS membranes and their nanocomposites counterparts with G and F nanofiller were analysed using a scanning electron microscope (FESEM, Leo Supra 55 – Zeiss Inc., Germany). Careful analysis of selected desired particles and features appearing in the morphological SEM images were carried out by using Image J analysis commercial software. It supports standard image J processing function such as contrast, sharpening, smoothing, and edge detection. The area of the pores selected in the morphological SEM images was calculated after all processing images were performed.

2.4. Pore Size Characterization. A porosimetry apparatus (Micromeritics Ins. Corp.) was used to measure nitrogen adsorption isotherms at 77.4 K. High purity (99.99%) nitrogen was used; before the measurement all samples were degassed at 300°C for 2 hrs. The instrument has two independent vacuum systems allowing simultaneous preparation of two samples and the analysis of the other. ASAP 2020 version 1.00 software included powerful data reduction to provide a variety of reports including pore volume, pore size, and pore surface area.

2.5. Permeability Characterization. Liquid permeability of the membranes was tested by passing NaOH solution through an inlet into a glass beaker containing phenolphthalein indicator that changes the color of the solution in the presence of NaOH from colorless to pink. A prototype composed of two polymeric parts, the top part (solution inlet) and the bottom part (solution outlet) as shown in Figure 2, was carefully designed and fabricated. The set-up was designed to have both top and bottom parts with central cylindrical holes in order to allow for the diffusion of NaOH solution passing through the membrane which was placed horizontally between the top cover and the bottom cup.

The time the NaOH solution took to pass through the porous membrane onto a glass beaker containing phenolphthalein indictor determined the permeability of each CS membrane. This is a preliminary set-up that was designed as a proof of concept.

2.5.1. Gas Permeability. Gas permeability determination was performed using the manometric method with permeability testing apparatus Type GDP-E (Brugger Feinmechanik GmbH). Monofilm material was analysed to determine

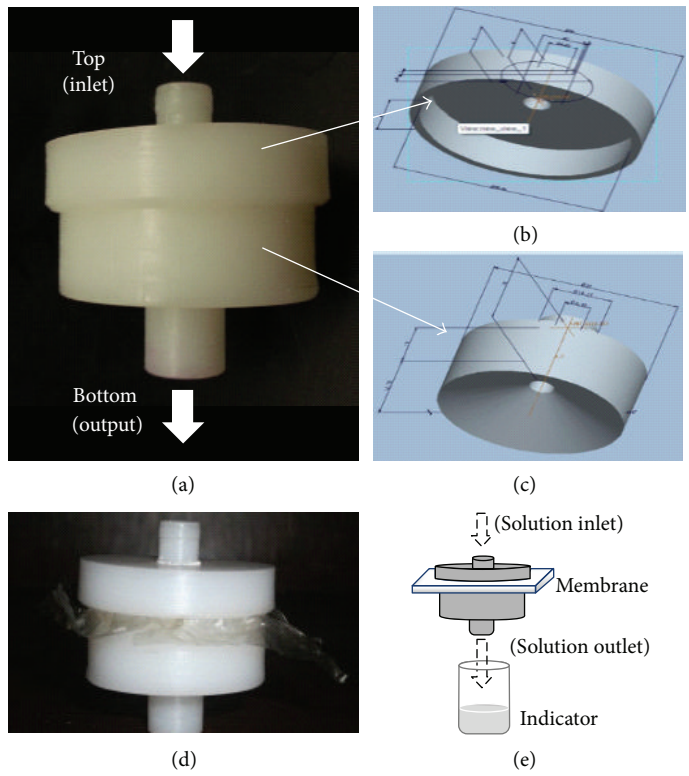

Figure 2: A schematic illustration of the designed set-up composed of two polymeric cylindrical parts for measuring liquid permeability of all fabricated CS membranes.

the permeability, diffusion, and solubility constants of the gas in the film. In this work, oxygen gas was used to prove the porosity of membranes. The oxygen permeability tests were performed three times for each type of sample to ensure reproducibility. The test was performed three times on an interval of three weeks to ensure the stability of the fabricated membranes as a function of time with no effect on the permeability of the membrane.

3. Results and Discussion

The main challenge behind manufacturing these novel CS nanocomposites mesoporous membranes lies in controlling their pore size to achieve precise separation capabilities of pollutants in order to decrease the amount of pollution. It has been shown that the pore size has a major effect on the properties of polymeric membranes. In the current work, the pore size varies according to the type (G versus F) and the amount (wt.%) of the added nanofillers materials to the polymer (chitosan) solution. Moreover, the variation of the pore size was affected by changing the chemical nature of the CS membranes by physical cross-linking of the CS membranes with TPP as a cross-linking agent.

3.1. Morphological Examination. The morphological examination of NCLCS and CLCS by SEM is illustrated in Figures 3(a) and 3(b), respectively, and clearly revealed a difference in the morphology between both images and the appearance of new porous network structure in case of CLCS after cross-linking with TPP as can be seen in Figure 3(b). These porous network structures were not observed in NCLCS and thus indicate the successful cross-linking of CS chains as has previously been reported [23]. These porous network structures of CLCS have also been observed in many morphological SEM images and were found to be stable at room temperature. A possible explanation for these porous networks is that the amino groups of CS react with the negative groups of TPP, thus establishing ionic interaction between CS chains. In addition, the effect of cross-linking could be explained as follows: the increase in length of the molecular chains between bonds upon cross-linking decreased the pore volume and surface area leading to a growth in the pore size [24].

Upon adding G and F nanofillers separately to NCLCS and CLCS solutions during the preparation step of the CS membranes as discussed in Section 2.2, the morphology of the SEM images changed significantly as compared to NCLCS. For example, as illustrated in Figure 3(a), the morphological SEM image of NCLCS shows a wide distribution of pores while upon adding G and F nanofillers with different wt.% (0.1 and 1%) as shown in Figures 4 and 5 (0.1 and 1% with G and F for NCLCS and CLCS), most of these pores were either decreased in size and/or decreased in number which is mostly due to the presence of the G and F nanofillers within the pores, thus leading to a decrease in the pore size. This observation has shown to have an effect on the barrier properties of the CS membranes as will be discussed in the following section. One can also see that the morphological

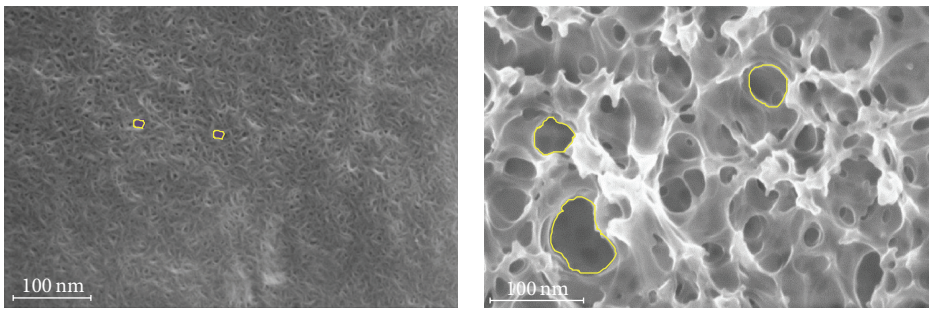

(a) (b)

Figure 3: Morphological SEM images (a) NCLCS and (b) CLCS, respectively. Different pores with different sizes are illustrated in color for display purposes.

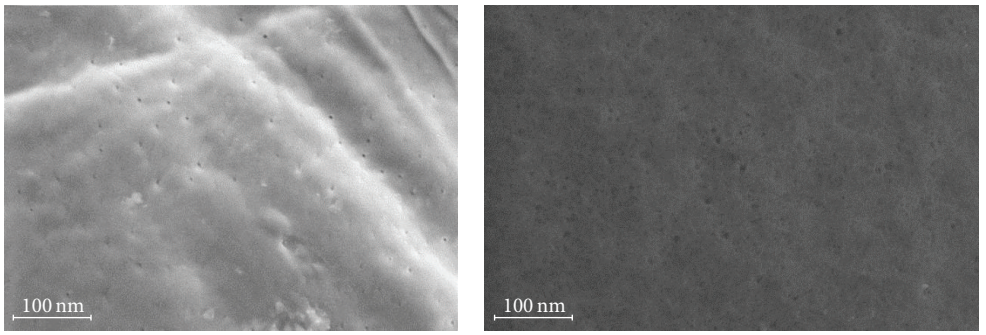

(a) (b)

Figure 4: Morphological SEM images of (a) NCLCS/0.1 wt.% G and (b) NCLCS/1 wt.% G.

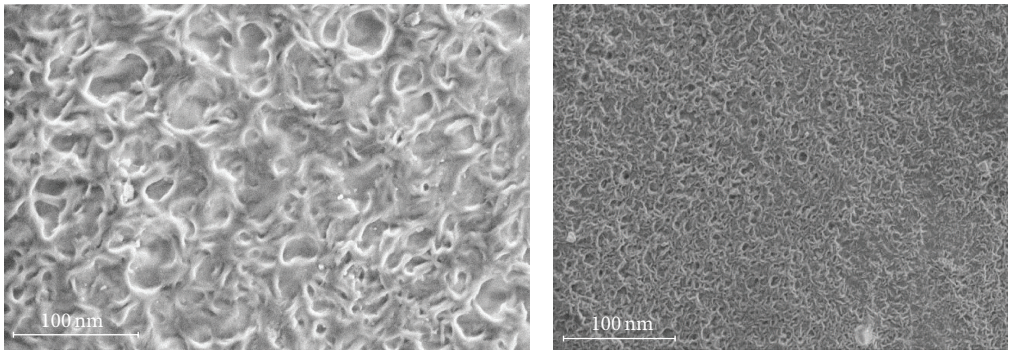

(a) (b)

Figure 5: Morphological SEM images of (a) NCLCS/0.1 wt.% F and (b) NCLCS/1 wt.% F.

change upon addition of G and F nanofillers can be better seen in the case of CLCS (Figures 6 of G and 7 with F, resp.). For display purposes, some of the pores of CLCS with G% with different sizes were colored as illustrated in Figure 6.

3.1.1. Pore Size Determination. The pore sizes of the CS membranes were calculated by two methods: (i) using ASAP 2020 software version 1.00 of the porosimeter's instrument which normally determines an average pore size of the features and not an individual pore size; the results observed from this software indicate an average pore size of 10 nm in case of NCLCS and 20 nm in case of CLCS, respectively, and (ii) using Image J analysis commercial software version 1.48 which allows the calculation of individual pore sizes from the recorded morphological SEM images, and not an average value as compared to the results obtained from ASAP 2020 software. Moreover, several morphological SEM images (large scale images and zoom-in areas) were used in the calculations in order to get more data about the pore size to be able to calculate the coefficient of variation (CV) which is the absolute value of relative standard deviation (RSD). Although the contrast and resolution of the morphological SEM images are not ideal to determine an accurate pore size especially in case of 2D surfaces such as the CS membranes;

Table 1: A comparison between the different CS membranes and their pore size at room temperature.

CS membranes	Average pore size (nm)	Stdv	Mean	CV (Stdv/mean)	Pore size % decrease
NCLCS	10	0.03	9.68	0.00	
NCLCS/0.1 wt G	3	0.03	2.40	0.01	0.70
NCLCS/1 wt G	2	0.04	0.31	0.11	0.80
NCLCS/0.1 wt F	5	0.03	4.48	0.01	0.44
NCLCS/1 wt F	4	0.03	3.44	0.01	0.56
CLCS	30	0.02	24.18	0.00	
CLCS/0.1 wt G	16	1.03	23.34	0.04	0.46
CLCS/1 wt G	10	0.05	8.65	0.01	0.66
CLCS/0.1 wt F	22	1.12	21.94	0.05	0.26
CLCS/1 wt F	20	0.03	17.40	0.00	0.33

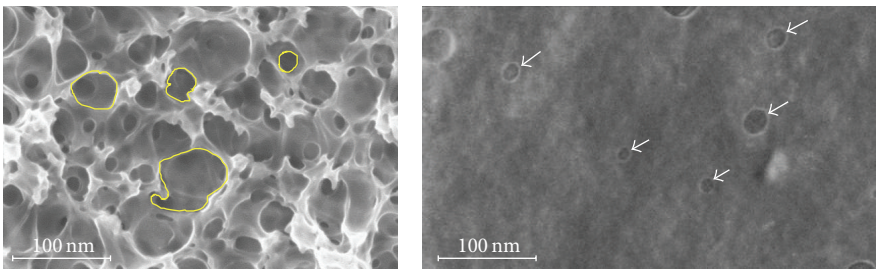

(a) (b)

Figure 6: Morphological SEM images of (a) CLCS/0.1 wt.% G and (b) CLCS/1 wt.% G.

however, the results obtained from both methods ((i) and (ii)) are complementary in nature and will certainly be useful to be compared in order to get more insights into the pore sizes of the CS membranes. The average pore size as determined by the porosimeter is illustrated in Table 1.

The pore size of the CS membranes as determined from the Image J analysis of the morphological SEM images is illustrated in Figure 8.

Table 1 illustrated the effect of increasing the wt.% of G nanofiller on the pores' size of the NCLCS membranes. At 0.1 wt.% G, the pores are obviously visible in the morphological SEM image as shown in Figures 4(a) and 8(c) with pore size mostly around 3 nm. However, by increasing the wt.% of G to 1%, the pore size reached mostly 2 nm. The 0.5 wt.% G showed similar pore size to the 1% G (data is not shown). Thus, by comparing the pore sizes of the CS membranes prepared by NCLCS versus NCLCS/0.1 wt.% G and NCLCS/1 wt.% G, there is a decrease in the pore size by 70% (with 0.1 wt.% G) and 80% (with 1 wt.% G), respectively. This is most probably due to the dispersion of graphene particles in between the chitosan polymer chains resulting in nearly blocking the CS membranes' pores. The barrier effect of nanofillers was confirmed in a review with exfoliated clay-based polymer nanocomposites, where nanoclay enhanced the barrier property of polymers [23].

Since the structure and chemical nature of the nanofiller is expected to affect their dispersion within the polymer matrix, F has been used as another nanofiller to be able to compare its effect with G nanofiller on the CS membranes' properties. Figure 5 showed the effect of increasing the wt.% of F nanofiller on the pores of the NCLCS membranes. At 0.1 wt.% F, the pores are quite visible with a pore size of 5 nm However, by increasing the wt.% to 1 wt.% F, the pore size reached 4 nm as suggested in the morphological SEM image in Figures 5(b) and 8(f). The 0.5% F showed similar pore size to the 1% F (data is not shown). Thus, by comparing the pore sizes of the CS membranes prepared by NCLCS versus NCLCS/0.1 wt.% F and NCLCS/1 wt.% F, there is a decrease in the pore size by 44% (with 0.1 wt.% F) and 56% (with 1 wt.% F), respectively. This is mainly due to the barrier effect of F which is not very efficient due to the small particle size of F (0.7–1 nm) with respect to the size of G nanofiller (6–8 nm). So far, we have clearly shown that the nanofiller type and wt.% plays a crucial role in controlling the pore size of CS membranes.

Figures 6, 8(g), and 8(h) suggested the effect of increasing the wt.% of G nanofiller on the pores of the CLCS membranes. At 0.1 wt.% G, the pores are quite visible mostly 20 nm in the morphological SEM image in Figure 6(a). However, the increase of G nanofiller to 1 wt.% reduces the pore size to mostly 10 nm with few larger pores as shown in the morphological SEM image. Thus, by comparing the pore sizes of the CS membranes prepared by CLCS versus CLCS/0.1 wt.% G and CLCS/1 wt.% G, there is a decrease in the pore size by 46% (with 0.1 wt.% G) and 66% (with 1 wt.% G), respectively. This is mainly due to the barrier properties of CLCS

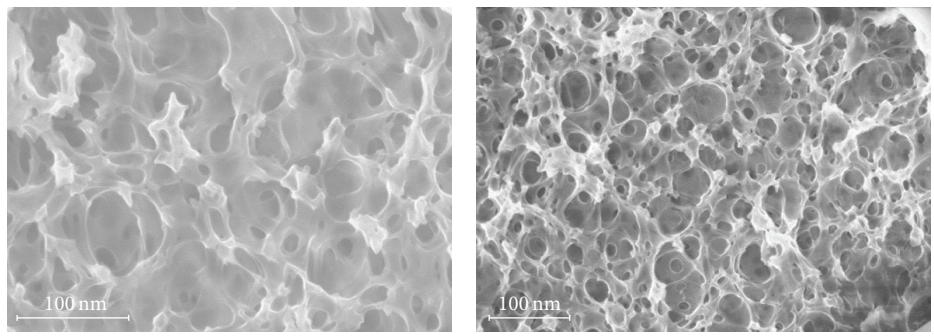

(a) (b)

Figure 7: Morphological SEM images of (a) CLCS/0.1 wt.% F and (b) CLCS/1 wt.% F.

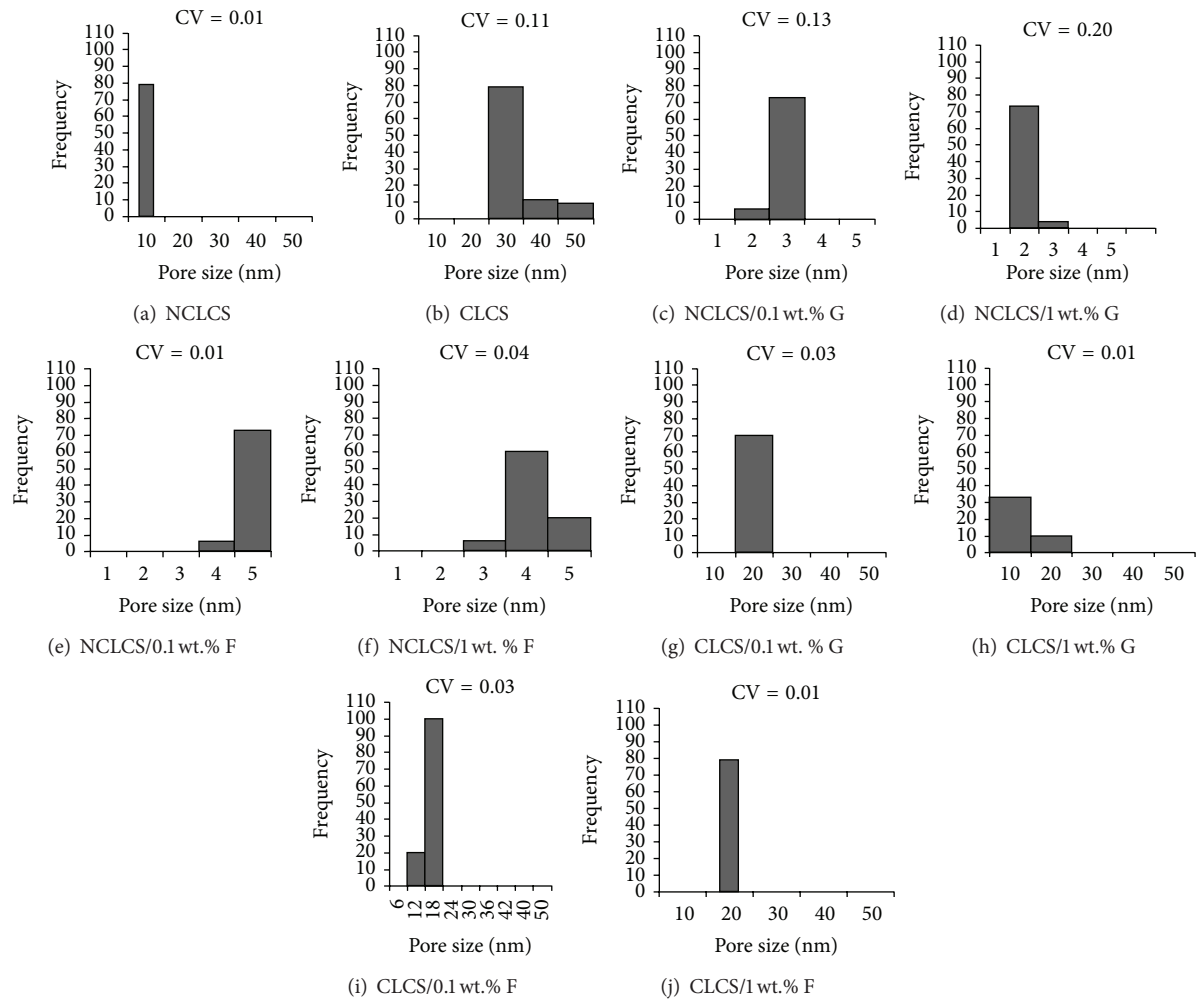

(a) NCLCS (b) CLCS (c) NCLCS/0.1 wt.% G (d) NCLCS/1 wt.% G

(e) NCLCS/0.1 wt.% F (f) NCLCS/1 wt. % F (g) CLCS/0.1 wt. % G (h) CLCS/1 wt.% G

(i) CLCS/0.1 wt.% F (j) CLCS/1 wt.% F

Figure 8: Pore size distribution of different CS membranes.

membranes which were significantly altered by the inclusion of G nanofiller that altered the diffusion path of penetrant molecules. Bharadwaj reported that, at high G nanofiller content in CLCS, significant decreases in permeability are predicted and observed in practice [25].

To compare the effect of the nanofiller on the properties of CLCS membranes, F was added to CS solutions in different wt.%. Table 1 and Figures 7, 8(i), and 8(j) showed the effect of increasing wt.% of F nanofiller on the pores of the CLCS membranes. At 0.1 wt.% F, the pores are quite visible mostly

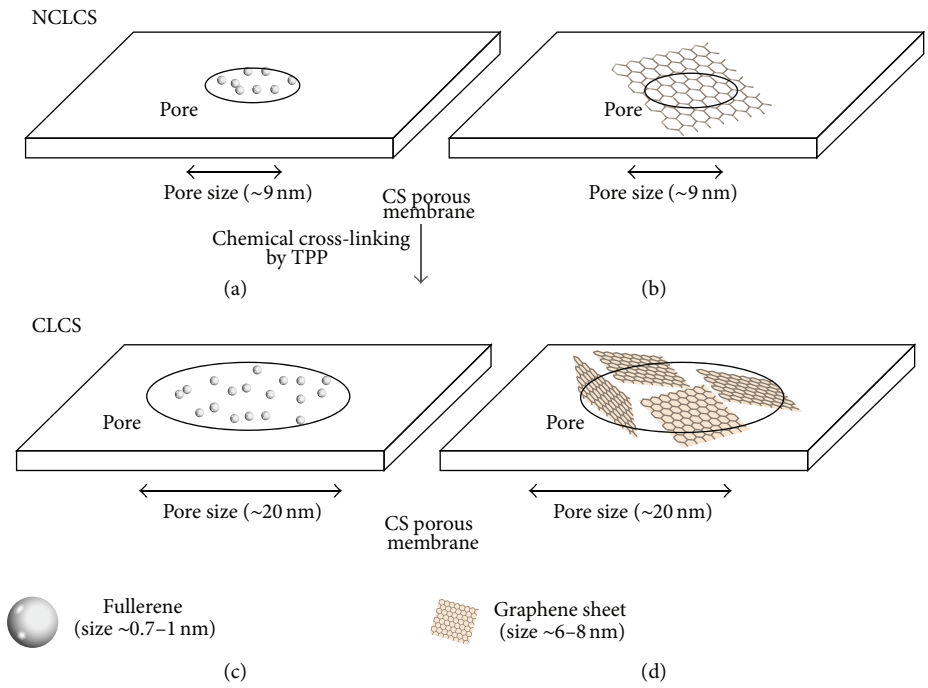

Figure 9: A schematic illustration of CS membranes and their pore sizes before and after physical cross-linking by TTP and after addition of F and G nanofillers at 23°C.

at 22 nm in the morphological SEM image in Figure 7(a). However, the increase of F nanofiller to 1 wt.% slightly reduced the pore size to 20 nm as shown in the morphological SEM image. The 0.5 wt.% F showed similar pore size to the 1% F (data is not shown). Thus, by comparing the pore sizes of the CS membranes prepared by CLCS versus CLCS/0.1 wt.% F and CLCS/1 wt.% F, there is a decrease in the pore size by 26% (with 0.1 wt.% F) and 33% (with 1 wt.% F), respectively.

3.2. Liquid Permeability. In order to measure the permeability of the fabricated CS membranes, diffusion time of NaOH was measured through each CS membrane. The diffusion time taken for NaOH to pass through the NCLC pores (16 hrs.) was longer than the diffusion time taken for NaOH to pass through CLC membranes (11 hrs.) due to the small diameter of the pores of NCLCS compared to CLCS membranes. Furthermore, the addition of 0.1 wt.% G to NCLCS membranes increased the diffusion time (20 hrs.) to pass through the pores in order to overcome the barrier effect of G. The increase of G to 1 wt.% increased the diffusion time to 25 hrs. However the barrier effect of F nanofiller was less than that of G. The diffusion of NaOH was faster in NCLCS membranes with 0.1 wt.% F (17 hrs.) compared with the CS membranes reinforced with G nanofiller. Moreover, increasing the wt.% of F nanofiller was found to increase the diffusion time (18 hrs.) due to the increase in barrier effect. The same effect of G and F addition to CLCS membranes occurred as diffusion time also increased but with a lower wt.% in CLCS/F membranes. Table 1 and Figure 8 summarized all the pore sizes of CS membranes as a result of adding different nanofillers (G and F) with different wt.% and as a result of cross-linking and mixing with G and F. One can clearly see the effect of decreasing the pore size is more obvious when using G nanofiller even with different wt.% as compared to F nanofiller with different wt.%.

From the above, one can conclude that the presence of G and F nanofillers inside the CS matrix affected the NaOH diffusion behaviour through the fabricated CS membranes. Diffusing molecules worked their way around impermeable particles, increasing path lengths, reducing mass transport rates, and improving barrier properties.

The pore size characteristics are very crucial in membrane industry, since these characteristics govern the filtration properties of the membrane. The NCLCS membranes have a pore size of 10 nm as shown in Figure 8. The addition of nanofillers (either G or F) decreased the pore size till 1.6 nm as the wt.% of the nanofiller increased to 1 wt.% as shown in Table 1. On the other hand, the addition of nanofillers to CLCS membranes decreased the pore size till 10 nm (with G) versus 22 nm (with F) as shown in Table 1. The barrier effect of G is found to be more than that of F due to the different size and structure between the two nanofillers as illustrated in the suggested scheme in Figure 9. G is in the form of flakes with a size of 6–8 nm while F has a spherical structure with a size of 0.7–1 nm. Figure 9 shows the cluster effect of G nanofiller on the CS pores that lead to their accumulation inside the pores of the CS membranes which leads to a decrease in the pore size of the CS membranes, whereas F nanofiller is dispersed inside the pores to an extent that allows higher permeability compared with G nanofiller. The pores in the scheme in Figure 9 have been scaled according to the obtained experimental pore sizes. Upon cross-linking of chitosan (CLCS membranes), the pore size increased from 10 nm to 30–50 nm as mentioned previously.

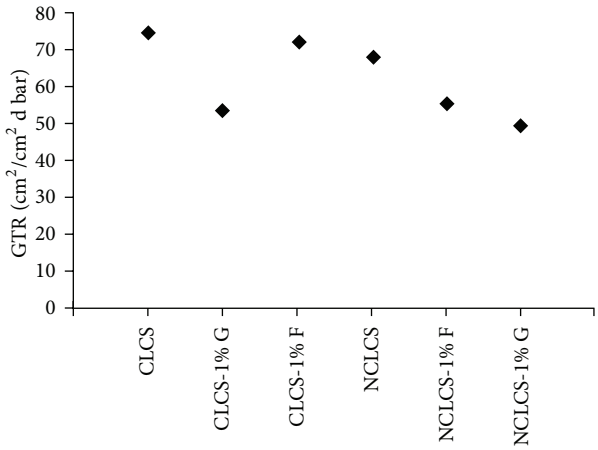

Figure 10: Oxygen transmission rate through different CS membranes.

3.3. Gas Permeability. The rate of oxygen transmission through the NCLCS membrane was 68 cm^2/cm^2 d bar. On the other hand, the increase in pore size in the CLCS membrane as a result of the cross-linking leads to an increase in the oxygen transmission rate reaching 75 cm^2/cm^2 d bar. Moreover, the addition of F nanofiller to the NCLCS membrane obtained a rate of 56 cm^2/cm^2 d bar due to the blocking effect of F to the CS membranes' pores. The blocking effect increased with the addition of F reaching a rate of 50 cm^2/cm^2 d bar. On the other hand, the addition of F to CLCS caused a blocking of the pores to a rate of 72 cm^2/cm^2 d bar and addition of G caused a low permeation rate reaching 52 cm^2/cm^2 d bar according to the increased barrier effect of G as shown in Figure 10.

In an attempt to highlight the filtration applications of the fabricated mesoporous membrane, sea salt (with a pore size of 35 nm) can be filtered using membranes CLCS membranes. Oil smoke (with a pore size of 30 nm) can be filtered using CLCS/0.1% F membranes. Smoke from combustion (with a pore size of 10 nm) could be filtered using NCLCS. Atmospheric dust (with a pore size of 1 nm) could be filtered using CLCS/0.5% G membranes. Oxygen and nitrogen (with a pore size of 0.5 nm) could be blocked using NCLCS/0.5% or 1% G [2].

4. Conclusion

In conclusion, the fabricated membranes are mesoporous; NCLCS membranes showed the formation of pore size of 10 nm, while CLCS membranes displayed 200% coarser pore sizes and 70% higher permeability. NCLCS and CLCS membranes reinforced with G and F nanofillers showed an improvement of the barrier properties compared to plain NCLCS, CLCS membranes. Work on the mechanical stability and improvement of the mechanical properties of the CS membranes upon the addition of nanofillers is currently in progress.

Conflict of Interests

The authors declare that there is no conflict of interests regarding the publication of this work.

Acknowledgments

The authors acknowledge the financial support received from the American University in Cairo (AUC) through Faculty Support Research Grant and also the Arab Academy for Science and Technology (ASRT), Egypt, through Ph.D. support grant.

References

[1] http://www.h2odistributors.com/chart-particle-sizes.asp.

[2] S. Kitagawa, R. Kitaura, and S.-I. Noro, "Functional porous coordination polymers," *Angewandte Chemie International Edition*, vol. 43, no. 18, pp. 2334–2375, 2004.

[3] J. Crank, *The Mathematics of Diffusion*, Clarendon Press, Oxford, UK, 2nd edition, 1975.

[4] L. Y. Ng, A. W. Mohammad, C. P. Leo, and N. Hilal, "Polymeric membranes incorporated with metal/metal oxide nanoparticles: a comprehensive review," *Desalination*, vol. 308, pp. 15–33, 2013.

[5] Information gathered from the official website of Sigma Aldrich, http://www.sigmaaldrich.com/catalog/product/sigma.

[6] K. Takita and S. Kikuchi, "Microporous polyolefin membrane, its production method, battery separator, and battery," US Patent no. US20090286161 A1, 2009, http://www.google.nl/patents/US20090286161?hl=nl&cl=ja.

[7] http://www.seipusa.com/products/w0200502.asp.

[8] P. Jollès and R. A. A. Muzzarelli, *Chitin and Chitinases*, Springer, Geneva, Switzerland, 1999.

[9] I. Siro and D. Plackett, *Nanocomposites for Food and Beverage Packaging. Principles and Practice*, Woodhead, Copenhagen, Denmark, 2012.

[10] M. N. V. R. Kumar, "A review of chitin and chitosan applications," *Reactive and Functional Polymers*, vol. 46, no. 1, pp. 1–27, 2000.

[11] X. Zeng and E. Ruckenstein, "Macroporous or microporous filtration," *Industrial and Engineering Chemistry Research*, vol. 43, pp. 708–711, 2004.

[12] W. He, X. Guo, L. Xiao, and M. Feng, "Study on the mechanisms of chitosan and its derivatives used as transdermal penetration enhancers," *International Journal of Pharmaceutics*, vol. 382, no. 1-2, pp. 234–243, 2009.

[13] R. A. A. Muzzarelli, "Genipin-crosslinked chitosan hydrogels as biomedical and pharmaceutical aids," *Carbohydrate Polymers*, vol. 77, no. 1, pp. 1–9, 2009.

[14] H. M. C. Azeredo, L. H. C. Mattoso, R. J. Avena-Bustillos et al., "Nanocellulose reinforced chitosan composite films as affected by nanofiller loading and plasticizer content," *Journal of Food Science*, vol. 75, no. 1, pp. N1–N7, 2010.

[15] F. N. Hafdani and N. Sadeghinia, "A review on application of chitosan as a natural antimicrobial," *World Academy of Science, Engineering and Technology*, vol. 50, pp. 252–256, 2011.

[16] A. K. Tiwary and V. Rana, "Cross-linked chitosan films: effect of cross-linking density on swelling parameters," *Pakistan Journal of Pharmaceutical Sciences*, vol. 23, no. 4, pp. 443–448, 2010.

[17] C. N. R. Rao, A. K. Sood, R. Voggu, and K. S. Subrahmanyam, "Some novel attributes of graphene," *Journal of Physical Chemistry Letters*, vol. 1, no. 2, pp. 572–580, 2010.

[18] K. B. Carey, T. Jerome, and S. Karna, "Carbon nanotube aluminium matrix nanocomposites," *Weapons and Materials Research Directorate*, *Army Research Laboratory*, vol. 1, 2010.

[19] D. V. Konarev, R. N. Lyubovskaya, N. V. Drichko et al., "Nanotechnology for implantable sensors: carbon nanotubes and graphene in medicine," *Journal of Materials Chemistry*, vol. 10, pp. 803–918, 2000.

[20] G. Gorrasi, M. Tortora, V. Vittoria et al., "Vapor barrier properties of polycaprolactone montmorillonite nanocomposites: effect of clay dispersion," *Polymer*, vol. 44, no. 8, pp. 2271–2279, 2003.

[21] J. Hosokawa, M. Nishiyama, K. Yoshihara, and T. Kubo, "Biodegradable film derived from chitosan and homogenized cellulose," *Industrials and Engineering Chemistry Research*, vol. 29, no. 5, pp. 800–805, 1990.

[22] S. B. Gudmund, A. Thorleif, and S. Paul, *Chitin and Chitosan: Sources, Chemistry, Biochemistry, Physical Properties, and Application*, Elsevier, London, UK, 1989.

[23] Q. Li, E. T. Dunn, E. W. Grandmaison, and M. F. A. Goosen, "Applications and properties of chitosan," *Journal of Bioactive and Compatible Polymers*, vol. 7, no. 4, pp. 370–397, 1992.

[24] E.-R. Kenawy, E. A. Kamoun, M. S. Mohy Eldin, and M. A. El-Meligy, "Physically crosslinked poly(vinyl alcohol)-hydroxyethyl starch blend hydrogel membranes: synthesis and characterization for biomedical applications," *Arabian Journal of Chemistry*, vol. 7, no. 3, pp. 372–380, 2014.

[25] R. K. Bharadwaj, "Modeling the barrier properties of polymer-layered silicate nanocomposites," *Macromolecules*, vol. 34, no. 26, pp. 9189–9192, 2001.